



Published in final edited form as:

*J Biomed Mater Res B Appl Biomater.* 2018 July ; 106(5): 1964–1975. doi:10.1002/jbm.b.34010.

## Hemocompatibility of Hyaluronan Enhanced Linear Low Density Polyethylene for Blood Contacting Applications

Rachael Simon-Walker<sup>1</sup>, John Cavicchia<sup>1</sup>, David A. Prawel<sup>1,2</sup>, Lakshmi Prasad Dasi<sup>3</sup>, Susan P. James<sup>1,2</sup>, and Ketul C. Popat<sup>1,2,\*</sup>

<sup>1</sup>School of Biomedical Engineering, Colorado State University, Fort Collins CO

<sup>2</sup>Department of Mechanical Engineering, Colorado State University, Fort Collins CO

<sup>3</sup>Department of Biomedical Engineering, Ohio State University, Columbus OH

### Abstract

Despite their overall success, different blood-contacting medical devices such as heart valves, stents, etc., are still plagued with hemocompatibility issues which often result in the need for subsequent replacement and/or life-long anticoagulation therapy. Consequently, there is a significant interest in developing biomaterials that can address these issues. Polymeric based materials have been proposed for use in many applications due to their ability to be finely tuned through manufacturing and surface modification to enhance hemocompatibility. In this study, we have developed a novel, hydrophilic biomaterial comprised of an interpenetrating polymer network (IPN) of hyaluronan (HA) and linear low density polyethylene (LLDPE). HA is a highly lubricous, anionic polysaccharide ubiquitously found in the human body. It is currently being investigated for a vast array of biomedical applications including cardiovascular therapies such as hydrogel based regenerative cell therapies for myocardial infarction, HA-coated stents, and surface modifications of polyurethane and metals for use in blood-contacting implants. The aim of this study was to assess the *in vitro* thrombogenic response of the hydrophilic polymer surface, HA-LLDPE for future potential use as flexible heart valve leaflets. The results indicate that HA-LLDPE is non-toxic and reduces thrombogenicity as compared to LLDPE surfaces, asserting its feasibility for use as a blood-contacting biomaterial.

### Keywords

blood-contacting biomaterials; hemocompatibility; thrombogenicity; hyaluronan

## INTRODUCTION

Hemostasis generated by contact with biomaterials involves a sophisticated interplay of blood constituents and enzymatic reactions resulting in the catalytic amplification of the coagulation cascade<sup>1–6</sup>. The recruitment of bulk phase components including plasma protein adsorption, platelet/leukocyte adhesion, activation, and aggregation, initiation of the contact system, and red blood cell hemolysis, all determine the degree to which these reactions are

\* Author for correspondence: ketul.popat@colostate.edu.

propagated. To mitigate these coagulation agonists, the manipulation of biomaterial surfaces has been widely investigated in hopes of achieving enhanced hemocompatibility of biomaterials. Some examples to enhance hemocompatibility include plasma surface modification, the grafting of oligo and poly(ethylene glycol)s (OEG, PEG), zwitterionic structures, heparin modification, the fabrication of PEGylated terpolymers, and the endothelialization of biomaterial surfaces<sup>1,3,7-19</sup>. Among the many techniques proposed to enhance hemocompatibility, much success has been found through the exploration of hyaluronan enhanced surfaces which have been shown to placate the hemostatic response<sup>12,14,20-24</sup>.

Hyaluronan (HA), a highly hydrophilic molecule, is a high molecular weight (HMW) polysaccharide found ubiquitously in the extracellular matrix of higher order mammals, and is considered nontoxic, biodegradable, and non-immunogenic<sup>21,25</sup>. It plays essential roles in tissue organization, cell proliferation, signaling reactions across the plasma membrane, and microbial virulence<sup>26</sup>. Hyaluronan is a known anticoagulant and has demonstrated an ability to stave off hemostasis on biomaterials. Hemocompatibility studies investigating immobilized HA coatings, multifunctional surface HA coatings, UV modified HA gels, and HA based hydrogel-antibody amalgamates have pointed to its ability to reduce plasma protein binding, platelet/leukocyte adhesion and activation, and related downstream events exacerbated by biomaterial surfaces<sup>20-24</sup>. However, these approaches have focused primarily on enhancing stent technology of metallic or hydrogel coated metal interfaces. Highly flexible and durable materials are needed for cardiovascular applications such as heart valve leaflets, vascular patches, and polymer applications which assist in creating biomimetic environments to modulate endothelialization and hemocompatibility. A recent review of HA and collagen IPN's for use in heart valve leaflets demonstrated the feasibility of developing a natural polymer IPN to mitigate hemostasis, yet these various developments resulted in HA degradation, low mechanical stability, or high cytotoxicity depending on the fabrication process<sup>27</sup>. Biomaterials for cardiovascular applications are required to be non-toxic, highly durable, and exhibit superior mechanical properties to resist shear stress.

To address the need for long-lasting, flexible, HA-enhanced, blood-contacting surfaces, a method for creating an "interpenetrating network" (IPN) of HMW-HA in linear low density polyethylene (LLDPE) was previously developed<sup>12</sup>. LLDPE was chosen for its high tensile and tear strength, and low bending stiffness, making it suitable for a wide range of cardiovascular applications including patches, grafts, and flexible heart valve leaflets. To achieve surface modification, virgin LLDPE was swollen in a solution of silyated-HA. The silyated-HA was subsequently cross-linked to itself before it was reverted to its native HA state via hydrolysis, thus creating a surface that is proposed to be anionic, hydrophilic, and hemocompatible. Previous investigation of hemolysis and platelet activation indicated that HA-LLDPE surfaces may reduce thrombotic proclivity as compared to virgin LLDPE and conventional heart valve materials including fixed tissue and pyrolytic carbon<sup>12</sup>. The purpose of this study was to characterize and comprehensively assess the hemocompatibility of LLDPE modified with 2% HA concentrated solution.

LLDPE surfaces enhanced using HMW-HA were characterized using attenuated total reflectance Fourier transform infrared spectroscopy (ATR-FTIR), contact angle and

thermogravimetric analysis (TGA). To determine whether the hemocompatibility of LLDPE was enhanced by the HMW-HA we assessed cytocompatibility, hemolysis, blood cell adhesion and activation, contact activation, fibrinogen binding, thrombin-antithrombin complex activation, and thrombin generation.

## Materials and Methods

### Fabrication of HA-LLDPE IPNs

HA/LLDPE IPN materials were manufactured using the swelling method described in detail elsewhere<sup>28–30</sup>. Briefly, sodium HA (~700 kDa, Lifecore Biomedical) was complexed with cetyltrimethylammonium (CTA) bromide to create HA-CTA, which was then silylated to create silylHA-CTA. The hydrophobic silylHA-CTA was introduced into the hydrophobic host (LLDPE) via swelling for 60 min in a hot (50°C) silylHA-CTA/xylene solution. The silylHA introduced into the LLDPE films was crosslinked with a 2% (v/v) poly(hexamethylene diisocyanate) (HMDI) xylenes solution. Treated LLDPE films were swelled at 50°C in a 2% (v/v) poly(hexamethylene diisocyanate) xylenes solution (i.e. HA crosslinking solution) for 60 min, and the crosslinker was cured in a vacuum oven at 50°C for 3 hr. Treated samples were then washed with acetone to remove excess HMDI and vacuum dried at room temperature until no change in weight was observed.

Because the silylHA was entangled at the molecular level and then crosslinked, the IPN survives hydrolysis (which converts the hydrophobic silylHA back into hydrophilic HA); i.e., the resulting hydrophilic HA cannot phase separate from the hydrophobic LLDPE. The details of hydrolysis are described in detail elsewhere<sup>31</sup>. Briefly, hydrolysis was performed by three successive 60 min ultrasonic baths in 0.2M NaCl solution (H<sub>2</sub>O:ethyl alcohol, 1:1) at 45°C, followed by 60 min of additional ultrasonication in pure 0.2M NaCl aqueous solution without ethyl alcohol, then washed twice in 3:2 H<sub>2</sub>O:ethyl alcohol solutions (first 2 hr, then 30 min), then dehydrated in acetone for 60 min, and finally dried under vacuum at 50°C until no change in weight was observed.

### Characterization of HA-LLDPE surfaces

HA-LLDPE surfaces were characterized using attenuated total reflectance Fourier transform infrared spectroscopy (ATR-FTIR) and thermogravimetric analysis. A Nicolet iS-50 FT-IR spectrometer with KBR beam splitter and diamond ATR crystal accessory was used to verify the presence of HA on the treated LLDPE films. Five spectra were taken with 4cm<sup>-1</sup> resolution with 64 scans per spectra at different sections on the film. Spectra were baseline corrected and averaged together for analysis.

A TGA 2950 (TA Instruments) was used for bulk-weight analysis of HA-LLDPE films. Between 4–6 mg of HA-LLDPE film was used per run and three runs were performed for each HA-LLDPE film. In a N<sub>2</sub> rich atmosphere, the samples were heated up to 600°C as follows:

- A heating rate of 25°C/min until a temperature of 110°C was reached, followed by an isothermal hold for 5mins to ensure any adsorbed water was evaporated.
- A heating rate of 10°C/min until a temperature of 540°C was reached.

- A heating rate of 25°C/min until a temperature of 600°C was reached, followed by an isothermal hold for 5mins.

The resulting thermograms were analyzed for weight % changes occurring between 150°C to 350°C, based on a calibration runs of samples with known amounts of cross-linked HA to be  $65 \pm 5\%$  of the true cross-linked amount of HA burned off in this temperature range. The final relative weight changes due to crosslinked HA were quantified as: (mean HA-LLDPE weight %) +  $0.35 * (\text{mean HA-LLDPE weight \%}) - \text{mean LLDPE weight \%}$  with the final standard error being  $\pm$  the square root of the sums of squared errors.

### **Platelet rich plasma isolation and incubation on different surfaces**

Whole human blood was drawn by a trained phlebotomist via venous phlebotomy from healthy donors who had refrained from taking thromboxane inhibitors (Ex: aspirin, ibuprofen, and naproxen) for at least 2 weeks. The protocol for blood isolation from healthy individuals was approved by Colorado State University Institutional Review Board. Blood was collected in BD vacutainer 2K EDTA tubes (Fischer Scientific). Platelet rich plasma (PRP) was isolated immediately following blood collection via centrifugation at 100 g for 15 mins and allowed to rest for 10 mins prior to use. PRP was pooled into a sterilized 50 ml conical tube. Polystyrene (PS, positive control), LLDPE (reference surface), and HA-LLDPE (investigative surface) (all 8mm in size) were placed into a 24-well plate and incubated with 1ml of pooled PRP on a horizontal shaker plate (100rpm) for 2hrs at 37°C and 5% CO<sub>2</sub>.

### **Material cytocompatibility**

Cytocompatibility was determined using a commercially available lactate dehydrogenase (LDH) assay kit (Cayman Chemical). Immediately following centrifugation and 10 mins rest, PRP was placed on the substrates. After 2 hrs of incubation in PRP, the surfaces were shaken on a horizontal shaker plate (100 rpm) for 5mins at room temperature. 100  $\mu$ L of surface-exposed PRP and manufacturer supplied standards were transferred to a 96-well plate. A reaction solution consisting of 96% v/v assay buffer, 1% v/v nicotinamide adenine dinucleotide NAD<sup>+</sup>1%, v/v lactic acid, 1% v/v INT, and 1% v/v LDH diaphorase was added in equal amounts (1:1) to all the standards and surface-exposed PRP. This was followed by gentle shaking on a horizontal shaker plate (100 rpm) for 30 mins at room temperature. Total time from blood collection to end of study was approximately 3 hrs. The absorbance of this was immediately measured at a wavelength of 490 nm using a plate reader (BMG Labtech).

### **Hemolysis on different surfaces**

Hemolysis on different surfaces was evaluated by measuring the amount of un-clotted blood on the surface after 2 hrs. Whole human blood was drawn by a trained phlebotomist via venipuncture from healthy donors who had refrained from taking thromboxane inhibitors for at least 2 weeks and placed into vacuum tubes without any anticoagulants. 5  $\mu$ L of blood was immediately placed onto the different surfaces and allowed to clot for up to 60 mins. To measure the amount of un-clotted blood, the surfaces were then transferred to a new 24-well plate after 15, 30, or 60 mins containing 500  $\mu$ L of DI water. The surfaces were then gently agitated for 30 secs on a shaker plate (100 rpm) and allowed to rest in DI water for 5 mins to

release any un-clotted blood from the surface. 200  $\mu$ L of the DI water/un-clotted blood solution was transferred to a 96-well plate and the absorbance was measured at a wavelength of 540 nm using a plate reader.

### Contact activation on different surfaces

Contact activation was assessed by an acid stop method (Chromogenix-S2302, DiaPharma) to investigate pre-kallikrein expression. The protocol provided by the manufacturer was followed. Immediately following blood collection and centrifugation PRP was administered to substrate surfaces. After 2 hrs of incubation, the surface-exposed PRP was diluted 10-fold in Tris buffer solution (pH 7.8). 100  $\mu$ l of the diluted PRP was then transferred to a 96-well plate and incubated at 37°C and 5% CO<sub>2</sub> for 3–4 mins. 100 $\mu$ l of pre-warmed (37°C) substrate solution was added to the wells and incubated at 37°C and 5% CO<sub>2</sub> for another 10mins. The reaction was stopped by adding 100  $\mu$ l of 20% acetic acid to the wells. PRP blanks were prepared by adding reagents in reverse order, without incubation. Total time of study from blood collection to end was approximately 3 hrs. The optical density of the solution was measured using a plate reader at 405 nm.

### Fibrinogen binding on different surfaces

Fibrinogen binding on different surfaces was assessed using an enzyme linked immunoassay (ELISA, GenWay). The protocol from the manufacturer was followed. After 2 hrs of incubation, the surface-exposed PRP was diluted (1:200) in the assay diluent. The diluted PRP and standards were transferred into the micro-assay well plate provided by the manufacturer and incubated for 60mins at room temperature. The PRP and standards were then aspirated and the wells were washed (4 $\times$ ) with wash buffer and incubated with enzyme antibody conjugate for 30 mins at room temperature in a dark environment. The conjugate was subsequently aspirated and the wells were washed (4 $\times$ ) with the wash buffer and incubated with a tetramethyl benzidine buffer (TMB) solution for 10 mins at room temperature in a dark environment. The approximate time length of the study from blood collection to end of study was 4 hrs. The reaction was stopped by adding stop solution and the optical density was immediately measured using a plate reader at 450nm.

### Plasma cell adhesion on different surfaces

PRP cell adhesion was investigated using fluorescence microscopy. Immediately after blood collection and centrifugation PRP was placed on substrates. After 2 hrs of incubation in PRP, the surfaces were stained with Calcein-AM (Thermo-scientific). The un-adhered cells were gently aspirated and the surfaces were rinsed with PBS (2 $\times$ ). 1ml of a 5 $\mu$ M solution of Calcein-AM in PBS was added to the surfaces. The surfaces were incubated for 20 mins in the stain solution. After 20 mins, the stain solution was gently aspirated and the surfaces rinsed with PBS (2 $\times$ ). The surfaces were immediately imaged using a Zeiss Axiovision fluorescent microscope using a 493/514 nm filter. All images were processed using Image J software. Total time from blood collection to imaging was approximately 2.5 hrs.

### **Platelet activation on different surfaces**

Platelet activation was determined using scanning electron microscopy (SEM). After blood collection, centrifugation and 2 hrs of incubation in PRP, surfaces were fixed with a primary fixative (6% glutaraldehyde (Sigma), 0.1M sodium cacodylate (Polysciences), and 0.1M sucrose (Sigma)) for 45 mins. The surfaces were then transferred to a secondary fixative (primary fixative without glutaraldehyde) for 10 mins. This was followed by exposing the surfaces to consecutive solutions of ethanol (35%, 50%, 70% and 100%) for 10 mins each. The surfaces were then air-dried and stored in a desiccator until imaging by SEM. Prior to imaging, the surfaces were coated with a 10 nm layer of gold and imaged at 5kV. Total time from blood collection to fixation was approximately 2.5 hrs.

### **Platelet factor 4 expression on different surfaces**

Platelet factor 4 (PF-4) expression was measured using an enzyme linked immunoabsorbant assay kit (ELISA, RayBio) to evaluate release from alpha granules during platelet activation. The protocol provided by the manufacturer was followed. Immediately following blood collection and centrifugation, PRP was distributed onto substrates. After 2 hrs of incubation, the surface-exposed PRP was diluted (1:200) in the assay diluent. The diluted PRP and standards were transferred into the micro-assay well plate and incubated for 2.5 hrs on a horizontal shaker plate (100 rpm) at room temperature. The PRP and standards were aspirated and the wells were washed (4×) with wash buffer and incubated with biotinylated antibody for 1 hr on a horizontal shaker plate (100 rpm) at room temperature. The antibody was then aspirated and the wells were washed (4×) to remove any unbound antibody. The wells were then incubated with a horseradish peroxidase (HRP)-streptavidin solution (1:25,000 in assay diluent) and incubated for 45 mins on a horizontal shaker plate (100 rpm) at room temperature. HRP was then aspirated and the wells were washed (4×) with wash buffer and incubated with TMB solution for 30 mins on a horizontal shaker plate (100 rpm) at room temperature in a dark environment. The reaction was stopped by adding stop solution and the optical density of was measured using a plate reader at 450 nm. Total time from blood collection to end of study was approximately 7 hrs.

### **Thrombin anti-thrombin (TAT) complex formation on different surfaces**

Thrombin anti-thrombin (TAT) complex formation was measured using a human thrombin anti-thrombin ELISA kit (HaemoScan). The protocol provided by the manufacturer was followed. A Nunc Maxisorp 96-well microtiter plate was coated with capture antibody and incubated in coating buffer overnight at 2–8°C. The plate was then washed (3×) with PBS-Tween wash buffer solution. Whole blood was drawn and immediately centrifuged and placed on the substrates. After 2 hrs of incubation, the surface-exposed PRP was diluted (1:200). 100 µL of diluted PRP and standards were transferred into the wells of the microtiter plate and incubated for 1 hr at room temperature. The PRP and controls were then aspirated and the wells were washed (3×) with wash buffer and incubated with 100 µl of antibody solution 1hr at room temperature. The wells were washed (3×) and 100 µl of substrate solution was added. After 20 mins, the reaction was stopped with 50 µl of stop solution and the optical density was measured using a plate reader at 450 nm. Total time from blood collection to end of study was approximately 4 hrs.

## Statistical Analysis

Each qualitative experiment was performed to evaluate the differences between PS, LLDPE and HA-LLDPE on at least three to five surfaces. Each assay was repeated at least three times with three different whole blood PRP populations ( $n_{\min} = 9$ ), except for ELISA's which were performed on at least five surfaces ( $n_{\min} = 15$ ) and hemolysis investigations which were performed on at least five surfaces ( $n_{\min} = 15$ ). Fluorescent imaging was performed using a Zeiss Axiovision fluorescent microscope at 10 $\times$  magnification and analyzed using ImageJ software. Percent coverage of platelets were determined by the evaluation of 15 representative images taken per group over 3 studies ( $n = 45$ ) using ImageJ. Each image covered an area of 25  $\mu\text{m}^2$ . Qualitative SEM analysis was performed using the methods described elsewhere on 15 representative images per group taken over 3 studies at 1000 $\times$  ( $n = 45$ )<sup>57</sup>. Each image covered an area of 144  $\mu\text{m}^2$ . All results were evaluated using a one-way analysis of variance (ANOVA) with a Tukey's, Bonferonni, and Scheffe post-hoc tests. Statistical significance was considered at  $p < 0.05$ .

## RESULTS AND DISCUSSION

Due to their high durability, flexible nature, and tunable surface properties, synthetic polymers such as LLDPE have been highly sought after for use as blood contacting materials<sup>7,32–35</sup>. Although relatively biocompatible, synthetic polymers used for cardiovascular applications remain susceptible to thrombosis due to their innate surface properties which are vastly different from native biological tissues<sup>36–38</sup>. In addition, this can be exacerbated in non-healthy patients that exhibit increased platelet activation such as those with coronary artery disease<sup>39</sup>. Exploration of HA enhanced surfaces suggest that HA can subdue stimulation of the hemostatic response<sup>12,21,24</sup>. Hemocompatibility studies investigating HA modifications of hydrogels and metals *in vitro* and *in vivo* have demonstrated the capacity for superior hemocompatibility derived from the anticoagulant and anionic nature of HA. However, these approaches have focused primarily on enhancing stent technology and have not addressed the need for flexible materials needed for wide-range cardiovascular applications. A recent review of HA and collagen IPNs for use in heart valve leaflets demonstrated the feasibility of a natural polymer IPN, yet these various developments resulted in HA degradation, low mechanical stability, or high cytotoxicity depending on the fabrication process<sup>27</sup>. Previous studies of 0.5%, 1%, and 1.5% initial solution concentrations of HA integrated into LLDPE resulted in a thin, flexible, and durable material that potentiates its use in a broad spectrum of cardiovascular applications. Lower hemolysis and reduced platelet activation was observed compared to virgin LLDPE and common HV materials used for both flexible leaflet and mechanical valves. Yet these studies were limited in their scope.

Biomaterials can facilitate the activation of the coagulation response by many routes. End products of blood-biomaterial interactions are determined by surface properties which drive protein adsorption and subsequent coagulatory enzyme catalysis, and blood cell adhesion. The initial sequestration of the material by the formation of a proteinated biofilm allows for signal mediation to occur between the implant and blood components leading to the exacerbation or mitigation of the hemostatic response. This can occur by two main

pathways; first, the adhesion of contact activation proteins which facilitate enzymatic catalysis of the intrinsic pathway; and secondly the adsorption of adhesive proteins such as fibrinogen which promotes subsequent attachment of platelets and leukocytes. Hemostatic responses to a biomaterial results from an overall combination of how these pathways are affected. Biomaterial surfaces can enact or subdue one or both pathways at any part of the overall cascade. In turn, the activation or pacification of one pathway can modulate the responses of the other. Thus, to understand how a surface may be affecting hemocompatibility it is essential to understand how the many components of the coagulation cascade are being influenced by its surface properties. Exploration of HA enhanced surfaces suggest that HA can subdue the activation of the hemostatic response<sup>12,14,19,22,23</sup>. In this study, we characterize the HA-LLDPE surface and investigate its effects on hemolysis, cytocompatibility, protein adhesion, cellular adhesion, and specific biochemical markers to gain a thorough understanding of the hematological response.

To confirm the presence of HA on LLDPE, ATR-FTIR spectra were taken for HA-LLDPE and compared to virgin LLDPE. The results indicate characteristic peaks for both HA and LLDPE on HA-LLDPE surfaces (Figure 1). The characteristic peaks for LLDPE include: CH<sub>3</sub> and CH<sub>2</sub> asymmetric and symmetric stretching near 2914 and 2847cm<sup>-1</sup>; CH<sub>2</sub> and CH<sub>3</sub> scissoring and stretching at 1472 and 1462cm<sup>-1</sup>; and CH<sub>2</sub> rocking at 718cm<sup>-1</sup>. The characteristics peaks for cross-linked HA include: OH and NH stretching near 3338cm<sup>-1</sup>; carbonyl stretching of urethane linkages near 1765cm<sup>-1</sup>; amide and carboxyl carbonyl stretching near 1685cm<sup>-1</sup>; and CNH stretching characteristic of amides and urethanes due to HA and the HMDI cross-linker near 152cm<sup>-1</sup>. Further, thermogravimetric analysis was used for bulk-weight analysis of HA-LLDPE surfaces. The results indicate a mean of 0.706 ± 0.379 w/v % of cross-linked HA in HA-LLDPE surfaces. The total standard error shown above includes the error propagated from the calibration procedure as well as the standard error from multiple samples. Thermogravimetric analysis is an imperfect tool for assessing the HA content in these samples. The HA-LLDPE films have numerous closely overlapping degradation temperatures which makes it necessary to use time consuming stepwise isothermal analysis if one wishes to see individual degradation products at specific degradation temperatures which must be added up to get the true value of crosslinked HA in the LLDPE matrix. To speed processing, the mean cumulative amount of crosslinked HA weight% change at 350°C was found to be, based on the average of three runs, 65±5%. This fact was used to estimate the true amount of crosslinked-HA in HA-LLDPE films.

Sample T-test between the HA-LLDPE and LLDPE treatment groups showed statistical significance at the 95% confidence level (p=0.001) between contact angles, with a mean of 28.3 ± 20 for HA-LLDPE and 86.8 ± 4.2 degrees for LLDPE, indicating a significant increase in the hydrophilicity of the LLDPE with HA enhancement.

To ensure that the inherent surface and material properties of HA-LLDPE posed no threats to the cellular components of blood, cytocompatibility was assessed using the prescribed protocol of a commercially available LDH assay kit. Results demonstrated no significant differences in cytotoxicity of HA-LLDPE, LLDPE, and PS surfaces (Figure 2). Cell membrane contact with toxic substances culminates in intracellular organelle swelling and rupturing leading to membrane permeabilization<sup>40</sup>. Cellular constituents, including LDH,



are then released into the extracellular milieu, allowing for the quantification of bulk cell necrosis through LDH assaying. PS is a well-known, non-toxic substance widely used in cell culture for its amenability toward cell preservation, growth, and differentiation. Similar LDH assay results to that of PS indicate that LLDPE and HA-LLDPE do not significantly result in any cytotoxic effects after 2hr contact with PRP.

To assess the amount of hemolysis on different surfaces, whole human blood was allowed to clot for 15, 30, and 60 mins on material surfaces. After each time point, the un-clotted blood was dissolved with DI water to lyse and release the hemoglobin of any red blood cells, which had not been trapped within the fibrin-matrix clot. Free hemoglobin was assessed using spectrophotometry with higher amounts of free hemoglobin indirectly indicating less clotting on the material surfaces. The results indicate that all the surfaces promoted some degree of hemolysis within 1 hr of exposure to whole blood. At all time points, the free hemoglobin for HA-LLDPE surfaces was significantly greater than that of PS and LLDPE illustrating that HA-LLDPE substantially reduced whole blood clotting (Figure 3, p **0.05**). In addition, total hemostasis was not observed on HA-LLDPE surfaces even after 1 hr of exposure to whole blood. However, both PS and LLDPE exhibited comparable levels of free hemoglobin at all time points, with total hemostasis observed after 1 hr of exposure to whole blood. Whole blood clotting assessments on material surfaces demonstrate the combined effects of pro-coagulant factors, platelet adhesion/activation, and contact activation thus offering an overview of the relationship between the surface properties and the biochemical reactions involved in the hemostatic response<sup>2</sup>. Material surface properties such as charge and hydrophilicity drive the physiological reactions by their amenability toward bulk phase elements implicated in the coagulation cascade. These include the specific make-up of the proteinated surface, the pro-coagulant status of platelets/leukocytes, the presence of pro-coagulant factors, and the amount by which the surface not covered by platelets activates the contact activation pathway. The specific combinations of these recruited and activated elements can then exacerbate, mediate, or equilibrate the catalytic amplification of thrombosis. While investigation of the individual components of the cascade can offer insight into the specific mechanisms by which the material surface invokes the amplification of the coagulation cascade, whole blood clotting offers the most clinically relevant index of thrombogenicity by presenting the combined effects of all components. Results of this study indicate that coagulation due to the specific combination of events significantly reduced thrombosis as compared to virgin LLDPE and PS. Further investigation of the interaction of the HA-LLDPE surface with individual components of the coagulation cascade was employed to determine the specific mechanisms by which blood clotting was attenuated on the surface.

Intrinsic pathway activation resulting from contact between blood and material surfaces is regulated by the adsorption of three zymogens; *Factor XII* which undergoes auto-activation upon contact with the surface triggering the cascade; *prekallikrein* which is cleaved by factor XII initiating a cascade amplifying positive feedback loop; and *high molecular weight kininogen*, a cofactor which assists in the activation of both prekallikrein and factor XII<sup>6,41-43</sup>. Although these zymogens work intimately together in the contact activation pathway, prekallikrein is the only one released into the plasma and can thus be most

accurately quantified to determine the magnitude of contact activation<sup>44</sup>. To investigate the effects of different surfaces on contact activation, an acid stop assay was used to determine the amount of prekallikrein expressed. The results exhibited no significant differences between LLDPE, HA-LLDPE, and PS. Although considered pro-coagulant in nature, PS is known to mitigate the activation of intrinsic pathway<sup>6</sup>. Comparing LLDPE and HA-LLDPE with that of PS demonstrates these surfaces may also inhibit contact activation (Figure 4). Previous studies suggest that polymers, similar to LLDPE, may be contact pathway suppressors. Hemocompatibility assessments of various polymers used for cardiovascular implants (e.g. Dacron, expanded polytetrafluoroethylene, and polyethylene) noted that factor XII remained inactive, thus halting the intrinsic pathway and retarding the cleavage of prekallikrein<sup>6,41,43</sup>. In addition, hemocompatibility studies performed with UV modified HA gels utilizing HMW-HA also determined that factor XII remained inactive. Thus, the combination of HMW-HA to LLDPE may further enhance the effect of polymer FXII activation suppression<sup>20</sup>. Factor XII inhibition is primarily based on how proteins adhere and activate on surfaces. Increases in surface hydrophobicity as seen on charged surfaces leads to competitive adsorption of plasma proteins not implicated in the coagulation cascade (e.g. albumin, IgG, transferrin), thus resulting in both inefficient binding of factor XII, and attenuated auto-activation of the protein<sup>45,46</sup>. In contrast, factor XII is known to easily bind to hydrophilic surfaces at a rate that is proportional with random “collisions” of the zygomen with the material surface which are sufficient in leading to protease autoactivation and downstream procoagulant activity<sup>45,46</sup>. However, surface functional groups of polymers containing carbonyl groups, such as those found within the HA-LLDPE network (Figure 1) exhibit relatively weak Lewis base interactions<sup>44</sup>. Weak Lewis bases are capable of hydrogen bonding to water and result in low-ion exchange across the surface. Strong carbonyl-hydrogen bonding, in this instance, may therefore hinder plasma proteins from effectively displacing interfacial water. Thus, lack of factor XII adhesion and auto-activation may be leading to similar mitigation of pre-kallikrein seen on LLDPE and PS surfaces<sup>44</sup>. Based on these results, it can be hypothesized that both LLDPE and HA-LLDPE have a similar role in attenuating intrinsic coagulation activity, by subduing the adsorption and activation of FXII albeit by different methods. To determine this further investigation would be required.

While many proteins exist within blood, (Ex: von Willebrand factor, albumin, vitronectin, fibronectin etc) fibrinogen binding is especially implicated in the regulation, adhesion, activation, and aggregation of circulating platelets to biomaterials. To characterize fibrinogen adsorption, surfaces were exposed to PRP for 2 hrs. PRP was then assayed to determine the amount of fibrinogen which remained within the plasma with greater amounts of free fibrinogen demonstrating less fibrinogen adsorption to the different surfaces. Significant differences were noted between the PS and LLDPE and HA-LLDPE surfaces ( $p < 0.05$ ) however, no significant difference in fibrinogen binding was noted between LLDPE and HA-LLDPE surfaces (Figure 5). Interfacial protein-surface interactions play a major role in coagulation responses<sup>39</sup>. Fibrinogen, in particular is a known agonist of pro-coagulant platelet adhesion, activation, and aggregation. Following surface adsorption, denatured fibrinogen spreads across the implant thereby increasing the surface area to which platelets can bind. Previous studies have shown a strong correlation between the rate and

amount of fibrinogen denaturation and the severity of inflammation and platelet adhesion making it important to assess the amount of fibrinogen which can bind to the HA-LLDPE surface<sup>5,47-49</sup>. Results of this study indicate that LLDPE and HA-LLDPE surfaces showed comparable fibrinogen adhesion. In this study EDTA chelated blood was used to assess protein adsorption. While EDTA anticoagulated blood may interfere with some mechanisms of the coagulation cascade such as complement activation, and platelet-fibrinogen binding, it does not interfere with the surface adsorption of proteins<sup>50,51</sup>. Polyethylene surfaces are known to preferentially bind the plasma protein albumin and can therefore mitigate the initial amount of fibrinogen bound to the LLDPE surface<sup>52</sup>. Furthermore, the molecular weight of HA determines its conformation and binding affinity to fibrinogen. HMW-HA is a known antagonist of fibrinogen only reacting with it after being cleaved to its low molecular weight form by the enzyme hyaluronidase<sup>53,54</sup>. Thus, the HMW of HA along with the integrated polyethylene structure may be responsible for the HA-LLDPE surface exhibiting a low binding affinity towards fibrinogen. In addition, the anionic nature of HA-LLDPE may have also reduced overall protein adhesion<sup>55,56</sup>. The results of the fibrinogen and contact activation studies indicate that thrombosis may be mitigated by the lack of procoagulant protein adhesion. Furthermore, the results indicate the both LLDPE and HMW-HA may be beneficial materials for use in cardiovascular implants.

The thrombotic proclivity of biomaterials is highly dependent on their ability to adhere and activate platelet and leukocytes, both through surface properties as well as by the creation of platelet micro-particles shed after contact with the surface<sup>1</sup>. In this study, platelet and leukocyte adhesion to different surfaces was characterized by fluorescence microscopy visualization after 2 hr of incubation followed by Calcein-AM staining. The images were processed and analyzed using ImageJ to determine total cell coverage on all surfaces. The results indicate significantly lower total cell adhesion on HA-LLDPE surfaces as compared to both PS and LLDPE (Figure 6(a)). The HA-LLDPE surfaces had approximately 76% and 83% less cell adhesion as compared to PS and LLDPE respectively (Figure 6(b),  $p < 0.05$ ). LLDPE surfaces exhibited greater cellular adhesion than HA-LLDPE even though fibrinogen adhesion was comparable (Figure 5). While EDTA anticoagulated blood is known to interfere with the interaction of platelets and fibrinogen by cleavage of the GPIIb/IIIa receptor, platelet adhesion to biomaterials can be modulated by many factors including adsorption of proteins that do not bind to the GPIIb/IIIa receptor, contact activation, and the material surface properties (Ex: wettability, surface roughness, and topography)<sup>57</sup>. Thus, platelet activation and adhesion to biomaterial surfaces in the presence of EDTA are driven mainly by the material surface properties, and not fibrinogen-platelet coupling. However, analysis of fibrinogen adsorption to the surface and platelet adhesion and activation studies show that HA-LLDPE significantly attenuates both responses inherent to the coagulation cascade and point to the propensity of HA-LLDPE to mitigate adverse coagulation as noted in the hemolysis studies. Although LLDPE did not promote significantly different amounts of fibrinogen adhesion as compared to HA-LLDPE its hydrophobic nature may result in increased amounts of cellular adhesion. The low amount of cellular adhesion to the HA-LLDPE surfaces indicates that it may mitigate ensuing thrombosis by limiting both platelet and leukocyte adhesion.

Although platelet adhesion to a surface can lead to a predilection for hemostasis, platelets must first be stimulated to become pro-coagulant. Five morphological variations of platelet dendritic expressions on implant surfaces have been identified and correspond with increasing levels of platelet activation: *round* (un-activated): disc shaped with no pseudopodia present; *dendritic* (partially activated): early pseudopodia i.e. short reversible dendritic extensions; *spread-dendritic* (moderately activated): irreversible long-dendritic extensions with some spreading and pseudopodial flattening; *spreading* (fully activated): pseudopodia almost fully flattened, with hyaloplasmic spreading; and *fully spread* (fully activated): no pseudopodia present, with full hyaloplasmic spreading<sup>58,59</sup>. SEM imaging was performed to visualize platelet activation on different surfaces. Similar to fluorescence microscopy images, SEM images also demonstrated significantly less cell adhesion on HA-LLDPE surfaces as compared to LLDPE and PS surfaces (Figure 7(a) and (b)). Further inspection of SEM images indicated that HA-LLDPE surfaces had the greatest number of platelets exhibiting round morphologies or slight reversible *dendritic* extensions with no aggregation. Very few platelets presented with *spread dendritic* morphologies. HA-LLDPE presented the least cellular adhesion to the surface. In contrast, LLDPE, and PS surfaces had similar amounts of platelet adhesion on the surface. LLDPE exhibited mostly *spread-dendritic* and some platelet aggregation. PS had the greatest amounts of platelets expressing *spreading* morphologies. EDTA has been found to activate platelets to some degree, similar to heparin and citrate, and is known to decrease platelet aggregation, making it useful for platelet counting<sup>60</sup>. Because of these effects, platelet activation on surfaces may be somewhat greater than what would be seen without the use of anticoagulants. Furthermore, platelet aggregation may have been reduced due to the use of EDTA. To quantify the amount of platelet activation, PF-4 assaying was performed in conjunction with qualitative assessments.

In conjunction with morphological changes, platelet degranulation releases dense granules and alpha granules, containing biomolecules (e.g. ADP, ATP, serotonin, and PF-4) which operate as chemokines and cytokines creating a positive feedback loop mobilizing further platelet activation. A PF-4 ELISA assay was performed to determine the effects of HA-LLDPE surfaces in triggering the release of PF-4 after incubation in PRP for 2 hrs. Results indicated no significant differences in PF-4 expression for platelets on LLDPE and HA-LLDPE surfaces however, PF-4 expression was significantly higher on PS surfaces therefore quantitatively confirming the results observed in fluorescent and SEM imaging (Figure 8, p 0.05). While platelet adhesion was higher on LLDPE surfaces they did not promote excessive activation as noted by their short dendritic extensions under SEM imaging and limited PF-4 expression. This further reinforces previous results that indicate LLDPE is a potentially a good base material for cardiovascular implants. In addition, lower platelet activation on HA-LLDPE surfaces further confirms a lessened proclivity for hemostasis due to reduced platelet recruitment and activation, most likely derived from its hydrophilic nature.

Upon initiation of the coagulation system, clotting factors are activated leading to a cascade of biochemical events which produce a fibrin matrix clot. These include the thrombin-antithrombin-complex (TAT), a protease inhibitor which binds to pro-thrombin resulting in cleavage units which can be quantified to assess thrombin activation and coagulation<sup>61,62</sup>.

Generation of the TAT complex after 2 hr of PRP incubation on different surfaces was determined by use of an enzyme immunoassay to evaluate the effects of substrates on surface coagulation. The results indicate no significant differences in TAT activation between all surfaces although trends indicate that PS resulted in higher TAT concentrations (Figure 9). These results are similar to other studies investigating thrombin generation on treated and untreated PS surfaces. While still considered pro-coagulant, untreated surfaces show less thrombin generation than oxygen, nitrogen, fluorine, and gamma treated PS. Comparing TAT activation on known hemocompatible surfaces such as silicone, Teflon, and star-PEG coated modified surfaces indicate TAT activation on LLDPE and HA-LLDPE surfaces are far below the generally recognized range for blood contacting interfaces considered to have excellent hemocompatibility properties<sup>1,62-65</sup>.

## CONCLUSION

The hemocompatibility of blood-contacting biomaterials is key to their success as cardiovascular implants. In this study, we evaluated the hemocompatibility of HA-LLDPE through use of cytocompatibility assays, contact activation, fibrinogen binding, TAT, and platelet adhesion and activation studies. HA-LLDPE was compared to unmodified LLDPE and PS, a known pro-coagulant surface. All the surfaces were found to be cytocompatible and did not induce significant cellular necrosis on platelets and leukocytes after 2 hrs of surface exposure. Whole blood clotting assays indicated that the HA-LLDPE surface significantly reduced clotting under static conditions. Subsequent evaluations of individual blood components determined that clotting results were likely due to a reduction of intrinsic pathway activation, platelet adhesion/activation, and mitigation of TAT complex scissions at the surface. None of the investigated surfaces significantly induced contact activation or TAT cleavage byproducts. While PS exhibited the highest amount of fibrinogen binding, which is a common indicator of platelet adhesion and activation, LLDPE and HA-LLDPE displayed similar amounts of fibrinogen adsorption at the surface. However, HA-LLDPE showed the lowest amounts of platelet adhesion and activation as compared to both LLDPE and PS. Overall, the results conclude that LLDPE may be a good base material for modifications amenable to increasing hemocompatibility. In this study, the enhancement of HA-LLDPE offered promising potential as a material which can be utilized for cardiovascular applications. Further studies are now directed towards development of surfaces with varying HA compositions and evaluating their hemocompatibility.

## Acknowledgments

Research reported in this publication was supported by National Heart, Lung and Blood Institute of the National Institutes of Health under award number R01HL119824.

## References

1. Gorbet MB, Sefton MV. Biomaterial-associated thrombosis: roles of coagulation factors, complement, platelets and leukocytes. *Biomaterials*. 2004; 25(26):5681–703. [PubMed: 15147815]
2. Grunkemeier JM, Tsai WB, Horbett TA. Hemocompatibility of treated polystyrene substrates: contact activation, platelet adhesion, and procoagulant activity of adherent platelets. *J Biomed Mater Res*. 1998; 41(4):657–70. [PubMed: 9697039]

3. Solouk A, Cousins BG, Mirzadeh H, Seifalian AM. Application of plasma surface modification techniques to improve hemocompatibility of vascular grafts: A review. *Biotechnol Appl Biochem*. 2011; 58(5):311–27. [PubMed: 21995534]
4. Tanaka KA, Key NS, Levy JH. Blood coagulation: hemostasis and thrombin regulation. *Anesth Analg*. 2009; 108(5):1433–46. [PubMed: 19372317]
5. Tang L, Lucas AH, Eaton JW. Inflammatory responses to implanted polymeric biomaterials: role of surface-adsorbed immunoglobulin G. *J Lab Clin Med*. 1993; 122(3):292–300. [PubMed: 8409705]
6. Vogler EA, Siedlecki CA. Contact activation of blood-plasma coagulation. *Biomaterials*. 2009; 30(10):1857–69. [PubMed: 19168215]
7. Ghanbari H, Viatge H, Kidane AG, Burriesci G, Tavakoli M, Seifalian AM. Polymeric heart valves: new materials, emerging hopes. *Trends Biotechnol*. 2009; 27(6):359–67. [PubMed: 19406497]
8. Huang N, Yang P, Leng YX, Chen JY, Sun H, Wang J, Wang GJ, Ding PD, Xi TF, Leng Y. Hemocompatibility of titanium oxide films. *Biomaterials*. 2003; 24(13):2177–87. [PubMed: 12699653]
9. Ikada Y, Iwata H, Horii F, Matsunaga T, Taniguchi M, Suzuki M, Taki W, Yamagata S, Yonekawa Y, Handa H. Blood compatibility of hydrophilic polymers. *J Biomed Mater Res*. 1981; 15(5):697–718. [PubMed: 12659136]
10. Jiang D, Liang J, Noble PW. Hyaluronan as an immune regulator in human diseases. *Physiol Rev*. 2011; 91(1):221–64. [PubMed: 21248167]
11. Mao C, Qiu Y, Sang H, Mei H, Zhu A, Shen J, Lin S. Various approaches to modify biomaterial surfaces for improving hemocompatibility. *Adv Colloid Interface Sci*. 2004; 110(1–2):5–17. [PubMed: 15142821]
12. Prawel DA, Dean H, Forleo M, Lewis N, Gangwish J, Popat KC, Dasi LP, James SP. Hemocompatibility and Hemodynamics of Novel Hyaluronan-Polyethylene Materials for Flexible Heart Valve Leaflets. *Cardiovasc Eng Technol*. 2014; 5(1):70–81. [PubMed: 24729797]
13. Stevens KN, Aldenhoff YB, van der Veen FH, Maessen JG, Koole LH. Bioengineering of improved biomaterials coatings for extracorporeal circulation requires extended observation of blood-biomaterial interaction under flow. *J Biomed Biotechnol*. 2007; 2007(10):29464. [PubMed: 18317517]
14. Verheye S, Markou CP, Salame MY, Wan B, King SB 3rd, Robinson KA, Chronos NA, Hanson SR. Reduced thrombus formation by hyaluronic acid coating of endovascular devices. *Arterioscler Thromb Vasc Biol*. 2000; 20(4):1168–72. [PubMed: 10764689]
15. Heath DE, Cooper SL. Design and characterization of sulfobetaine-containing terpolymer biomaterials. *Acta Biomater*. 2012; 8(8):2899–910. [PubMed: 22503950]
16. Hoshi RA, Van Lith R, Jen MC, Allen JB, Lapidus KA, Ameer G. The blood and vascular cell compatibility of heparin-modified ePTFE vascular grafts. *Biomaterials*. 2013; 34(1):30–41. [PubMed: 23069711]
17. Jantzen AE, Noviani M, Mills JS, Baker KM, Lin FH, Truskey GA, Achneck HE. Point-of-care seeding of nitinol stents with blood-derived endothelial cells. *J Biomed Mater Res B Appl Biomater*. 2016; 104(8):1658–1665. [PubMed: 26340233]
18. Shemesh D, Goldin I, Hijazi J, Zaghali I, Berelowitz D, Verstandig A, Olsha O. A prospective randomized study of heparin-bonded graft (Propaten) versus standard graft in prosthetic arteriovenous access. *J Vasc Surg*. 2015; 62(1):115–22. [PubMed: 25770987]
19. Wang W, Zheng Z, Huang X, Fan W, Yu W, Zhang Z, Li L, Mao C. Hemocompatibility and oxygenation performance of polysulfone membranes grafted with polyethylene glycol and heparin by plasma-induced surface modification. *J Biomed Mater Res B Appl Biomater*. 2016
20. Amarnath LP, Srinivas A, Ramamurthi A. In vitro hemocompatibility testing of UV-modified hyaluronan hydrogels. *Biomaterials*. 2006; 27(8):1416–24. [PubMed: 16143386]
21. Camci-Unal G, Aubin H, Ahari AF, Bae H, Nichol JW, Khademhosseini A. Surface-modified hyaluronic acid hydrogels to capture endothelial progenitor cells. *Soft Matter*. 2010; 6(20):5120–5126. [PubMed: 22368689]
22. Thierry B, Winnik FM, Merhi Y, Griesser HJ, Tabrizian M. Biomimetic hemocompatible coatings through immobilization of hyaluronan derivatives on metal surfaces. *Langmuir*. 2008; 24(20):11834–41. [PubMed: 18759386]

23. Thierry B, Winnik FM, Merhi Y, Silver J, Tabrizian M. Radionuclides-hyaluronan-conjugate thromboresistant coatings to prevent in-stent restenosis. *Biomaterials*. 2004; 25(17):3895–905. [PubMed: 15020166]
24. Wu F, Li J, Zhang K, He Z, Yang P, Zou D, Huang N. Multifunctional Coating Based on Hyaluronic Acid and Dopamine Conjugate for Potential Application on Surface Modification of Cardiovascular Implanted Devices. *ACS Appl Mater Interfaces*. 2016; 8(1):109–21. [PubMed: 26654689]
25. Laurent TC, Laurent UB, Fraser JR. The structure and function of hyaluronan: An overview. *Immunol Cell Biol*. 1996; 74(2):A1–7. [PubMed: 8724014]
26. Hascall, V., Esko, JD. Hyaluronan. In: Varki, A.Cummings, RD.Esko, JD.Freeze, HH.Stanley, P.Bertozzi, CR.Hart, GW., Etzler, ME., editors. *Essentials of Glycobiology*. Cold Spring Harbor (NY): 2009.
27. Nazir R. Collagen–hyaluronic acid based interpenetrating polymer networks as tissue engineered heart valve. *Materials Science and Technology*. 2016; 32(9):871–882.
28. James, SPGBMZ. Outer Layer Having Entanglement of Hydrophobic Polymer Host and Hydrophilic Polymer Guest. USA patent. 7,662,954. 2010. Feb 16. 2010
29. Zhang M, James SP, Rentfrow E. The effect of IPN treatment on the mechanical properties of UHMWPE. *Biomedical Sciences Instrumentation*. 2001; 37:7–12. [PubMed: 11347448]
30. Dean, HC. Development of a Biopoly™ Micro-composite For Use In Prosthetic Heart Valve Replacements. Fort Collins: Colorado State University; 2011. **Master of Science**
31. Zhang M, Pare P, King R, James SP. A novel ultra high molecular weight polyethylene-hyaluronan microcomposite for use in total joint replacements. II. Mechanical and tribological property weight ocomposite for evaluation. *Journal of Biomedical Materials Research Part A*. 2007; 82A(1):18–26.
32. Courtney JM, Lamba NM, Sundaram S, Forbes CD. Biomaterials for blood-contacting applications. *Biomaterials*. 1994; 15(10):737–44. [PubMed: 7986936]
33. Hayward JA, Chapman D. Biomembrane surfaces as models for polymer design: the potential for haemocompatibility. *Biomaterials*. 1984; 5(3):135–42. [PubMed: 6375749]
34. Ishihara K, Iwasaki Y, Ebihara S, Shindo Y, Nakabayashi N. Photoinduced graft polymerization of 2-methacryloyloxyethyl phosphorylcholine on polyethylene membrane surface for obtaining blood cell adhesion resistance. *Colloids Surf B Biointerfaces*. 2000; 18(3–4):325–335. [PubMed: 10915954]
35. Wu WI, Sask KN, Brash JL, Selvaganapathy PR. Polyurethane-based microfluidic devices for blood contacting applications. *Lab Chip*. 2012; 12(5):960–70. [PubMed: 22273592]
36. Hecker JF, Scandrett LA. Roughness and thrombogenicity of the outer surfaces of intravascular catheters. *J Biomed Mater Res*. 1985; 19(4):381–95. [PubMed: 4055822]
37. Pottecher T, Forrler M, Picardat P, Krause D, Bellocq JP, Otteni JC. Thrombogenicity of central venous catheters: prospective study of polyethylene, silicone and polyurethane catheters with phlebography or post-mortem examination. *Eur J Anaesthesiol*. 1984; 1(4):361–5. [PubMed: 6536520]
38. Stabile E, Cheneau E, Kinnaird T, Suddath WO, Weissman NJ, Torguson R, Kent KM, Pichard AD, Satler LF, Waksman R. Late thrombosis in cypher stents after the discontinuation of antiplatelet therapy. *Cardiovasc Radiat Med*. 2004; 5(4):173–6. [PubMed: 16237987]
39. Braune S, Gross M, Walter M, Zhou S, Dietze S, Rutschow S, Lendlein A, Tschöpe C, Jung F. Adhesion and activation of platelets from subjects with coronary artery disease and apparently healthy individuals on biomaterials. *J Biomed Mater Res B Appl Biomater*. 2016; 104(1):210–7. [PubMed: 25631281]
40. Chan FK, Moriwaki K, De Rosa MJ. Detection of necrosis by release of lactate dehydrogenase activity. *Methods Mol Biol*. 2013; 979:65–70. [PubMed: 23397389]
41. Cool DE, Edgell CJ, Louie GV, Zoller MJ, Brayer GD, MacGillivray RT. Characterization of human blood coagulation factor XII cDNA. Prediction of the primary structure of factor XII and the tertiary structure of beta-factor XIIa. *J Biol Chem*. 1985; 260(25):13666–76. [PubMed: 3877053]
42. Konings J, Govers-Riemslog JW, Philippou H, Mutch NJ, Borissoff JI, Allan P, Mohan S, Tans G, Ten Cate H, Ariens RA. Factor XIIa regulates the structure of the fibrin clot independently of

thrombin generation through direct interaction with fibrin. *Blood*. 2011; 118(14):3942–51. [PubMed: 21828145]

43. Schmaier AH. Contact activation: a revision. *Thromb Haemost*. 1997; 78(1):101–7. [PubMed: 9198136]
44. Girey GJ, Talamo RC, Colman RW. The kinetics of the release of bradykinin by kallikrein in normal human plasma. *J Lab Clin Med*. 1972; 80(4):496–505. [PubMed: 4627469]
45. Chatterjee K, Guo Z, Vogler EA, Siedlecki CA. Contributions of contact activation pathways of coagulation factor XII in plasma. *J Biomed Mater Res A*. 2009; 90(1):27–34. [PubMed: 18481791]
46. Josh Yeh CH, Dimachkie ZO, Golas A, Cheng A, Parhi P, Vogler EA. Contact activation of blood plasma and factor XII by ion-exchange resins. *Biomaterials*. 2012; 33(1):9–19. [PubMed: 21982294]
47. Rubens F, Brash J, Weitz J, Kinlough-Rathbone R. Interactions of thermally denatured fibrinogen on polyethylene with plasma proteins and platelets. *J Biomed Mater Res*. 1992; 26(12):1651–63. [PubMed: 1484068]
48. Skarja GA, Brash JL, Bishop P, Woodhouse KA. Protein and platelet interactions with thermally denatured fibrinogen and cross-linked fibrin coated surfaces. *Biomaterials*. 1998; 19(23):2129–38. [PubMed: 9884053]
49. Tang L, Eaton JW. Inflammatory responses to biomaterials. *Am J Clin Pathol*. 1995; 103(4):466–71. [PubMed: 7726145]
50. Engberg AE, Rosengren-Holmberg JP, Chen H, Nilsson B, Lambris JD, Nicholls IA, Ekdahl KN. Blood protein-polymer adsorption: implications for understanding complement-mediated hemoincompatibility. *J Biomed Mater Res A*. 2011; 97(1):74–84. [PubMed: 21319295]
51. Geffken DF, Keating FG, Kennedy MH, Cornell ES, Bovill EG, Tracy RP. The measurement of fibrinogen in population-based research. Studies on instrumentation and methodology. *Arch Pathol Lab Med*. 1994; 118(11):1106–9. [PubMed: 7526817]
52. Baszkin A, Boissonnade MM. Competitive Adsorption of Albumin and Fibrinogen at Solution?Air and Solution?Polyethylene Interfaces. *Proteins at Interfaces II*. American Chemical Society. 1995:209–227.
53. Bonafe F, Govoni M, Giordano E, Caldarera CM, Guarnieri C, Muscari C. Hyaluronan and cardiac regeneration. *J Biomed Sci*. 2014; 21:100. [PubMed: 25358954]
54. Ruppert SM, Hawn TR, Arrigoni A, Wight TN, Bollyky PL. Tissue integrity signals communicated by high-molecular weight hyaluronan and the resolution of inflammation. *Immunol Res*. 2014; 58(2–3):186–92. [PubMed: 24614953]
55. Eriksson C, Nygren H. Polymorphonuclear leukocytes in coagulating whole blood recognize hydrophilic and hydrophobic titanium surfaces by different adhesion receptors and show different patterns of receptor expression. *J Lab Clin Med*. 2001; 137(4):296–302. [PubMed: 11283525]
56. Leszczak V, Popat KC. Improved in vitro blood compatibility of polycaprolactone nanowire surfaces. *ACS Appl Mater Interfaces*. 2014; 6(18):15913–24. [PubMed: 25184556]
57. Fatisson J, Mansouri S, Yacoub D, Merhi Y, Tabrizian M. Determination of surface-induced platelet activation by applying time-dependency dissipation factor versus frequency using quartz crystal microbalance with dissipation. *J R Soc Interface*. 2011; 8(60):988–97. [PubMed: 21247945]
58. Goodman SL, Grasel TG, Cooper SL, Albrecht RM. Platelet shape change and cytoskeletal reorganization on polyurethaneureas. *J Biomed Mater Res*. 1989; 23(1):105–23.
59. Ko T-M, Cooper SL. Surface properties and platelet adhesion characteristics of acrylic acid and allylamine plasma-treated polyethylene. *Journal of Applied Polymer Science*. 1993; 47(9):1601–1619.
60. Macey M, Azam U, McCarthy D, Webb L, Chapman ES, Okrongly D, Zelmanovic D, Newland A. Evaluation of the anticoagulants EDTA and citrate, theophylline, adenosine, and dipyridamole (CTAD) for assessing platelet activation on the ADVIA 120 hematology system. *Clin Chem*. 2002; 48(6 Pt 1):891–9. [PubMed: 12029005]
61. Chandler WL, Velan T. Estimating the rate of thrombin and fibrin generation in vivo during cardiopulmonary bypass. *Blood*. 2003; 101(11):4355–62. [PubMed: 12480702]



62. Muthusubramaniam L, Lowe R, Fissell WH, Li L, Marchant RE, Desai TA, Roy S. Hemocompatibility of silicon-based substrates for biomedical implant applications. *Ann Biomed Eng.* 2011; 39(4):1296–305. [PubMed: 21287275]
63. Hong J, Nilsson Ekdahl K, Reynolds H, Larsson R, Nilsson B. A new in vitro model to study interaction between whole blood and biomaterials. Studies of platelet and coagulation activation and the effect of aspirin. *Biomaterials.* 1999; 20(7):603–11. [PubMed: 10208402]
64. Schleicher M, Hansmann J, Elkin B, Kluger PJ, Liebscher S, Huber AJ, Fritze O, Schille C, Muller M, Schenke-Layland K, et al. Oligonucleotide and Parylene Surface Coating of Polystyrene and ePTFE for Improved Endothelial Cell Attachment and Hemocompatibility. *Int J Biomater.* 2012; 2012:397813. [PubMed: 22481939]
65. van der Kamp KW, Hauch KD, Feijen J, Horbett TA. Contact activation during incubation of five different polyurethanes or glass in plasma. *J Biomed Mater Res.* 1995; 29(10):1303–6. [PubMed: 8557733]

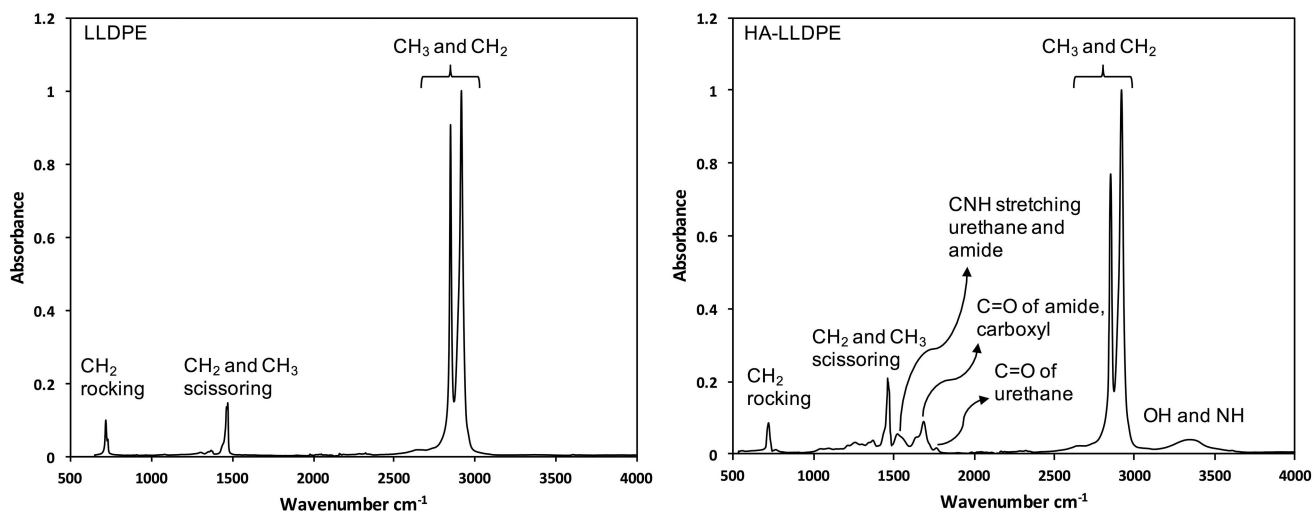


**Figure 1.**  
ATR-FTIR spectra for LLDPE and HA-LLDPE surfaces showing characteristic peaks.

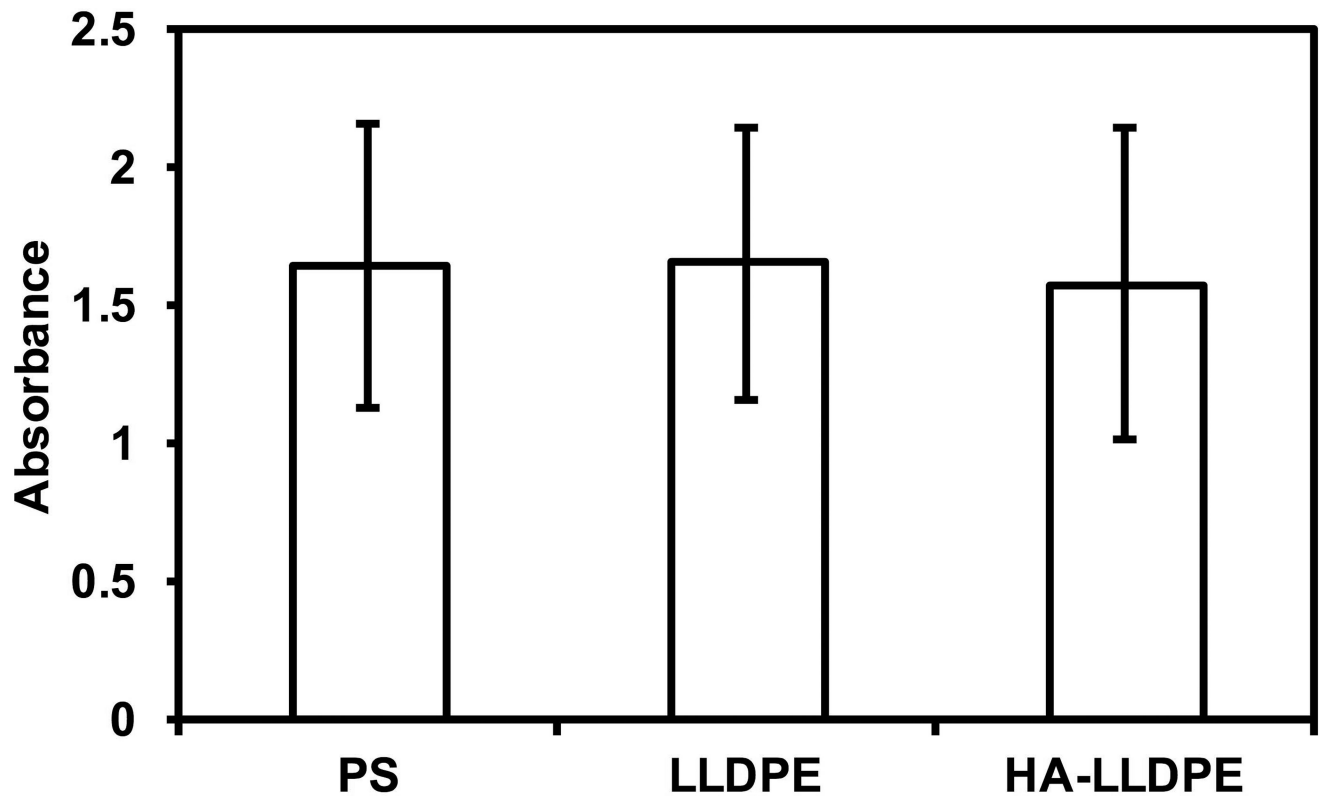


**Figure 2.**

Cytotoxicity of different material surfaces assessed after 2 hrs of incubation in whole blood plasma. Results indicate no significant difference in LDH activity for all surfaces.

Experiments were replicated with at least three different cell populations on at least three different samples ( $n_{\min} = 9$ ).

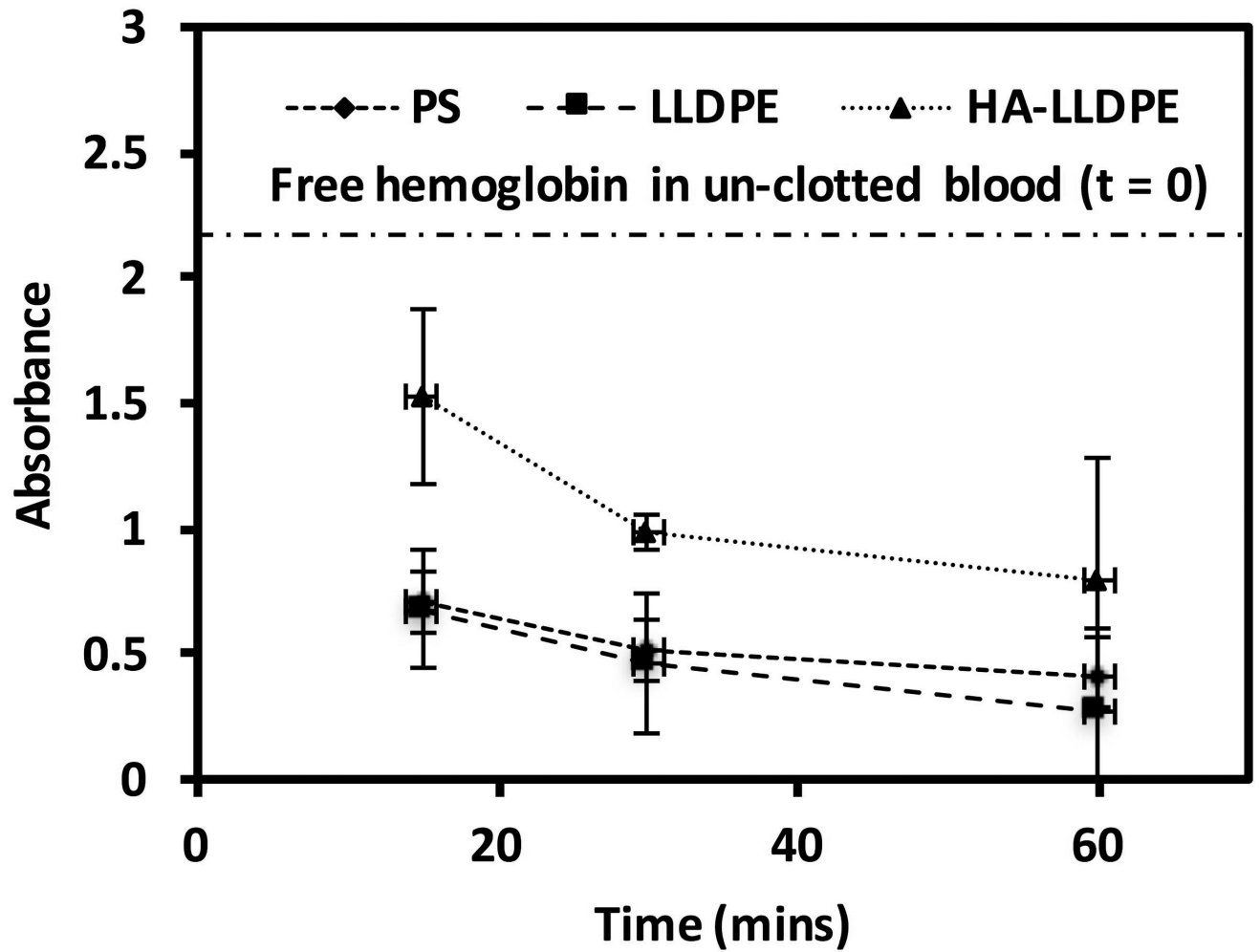


**Figure 3.** Free hemoglobin concentration as determined by absorbance on PS, LLDPE, and HA-LLDPE surfaces. Significant differences in free hemoglobin concentrations were seen between HA-LLDPE and all other surfaces at all time points. No significance was seen between PS and LLDPE  $p < 0.05$ .

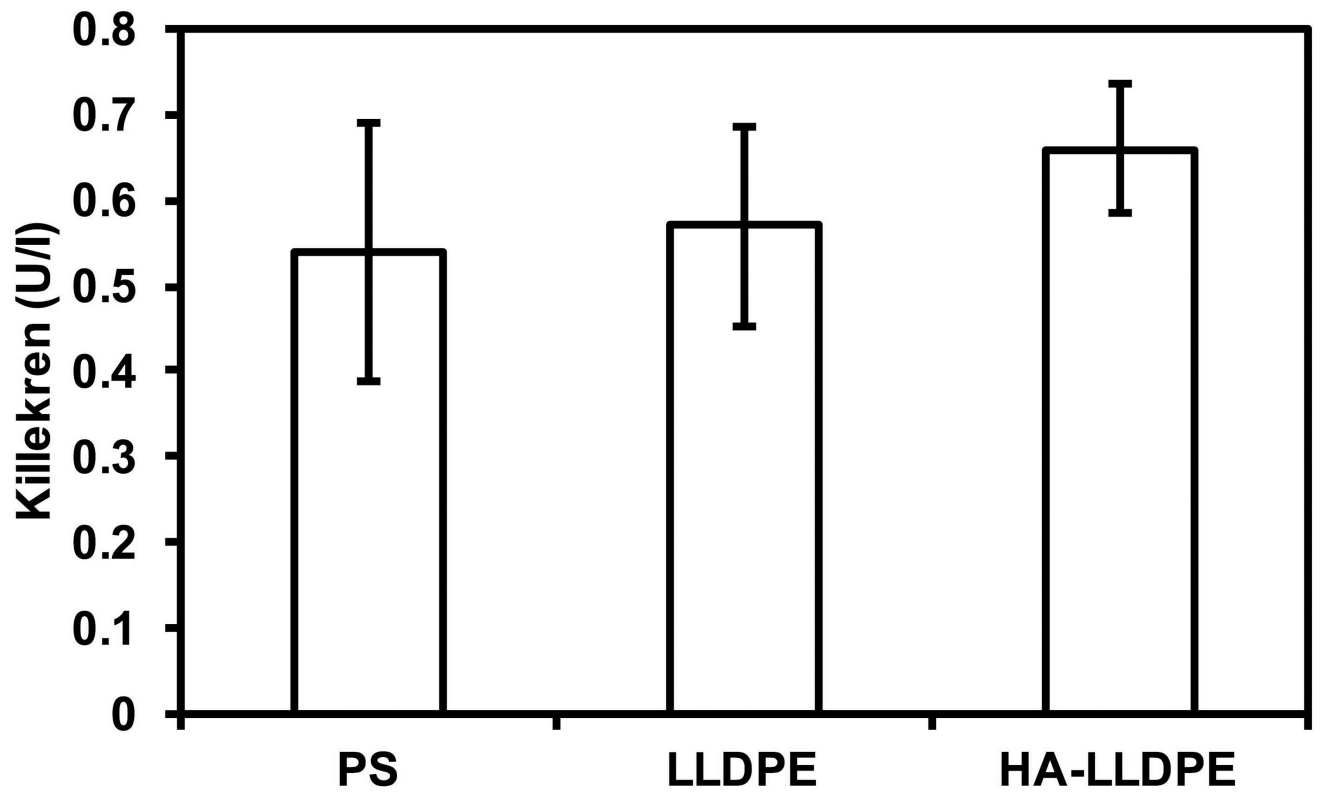


**Figure 4.**

Contact activation measured by the amount of pre-kallikrein on different surfaces after 2 hrs of incubation in whole plasma. The results indicate no significant difference in contact activation on the surfaces. Experiments were replicated with at least three different cell populations on at least three different samples ( $n_{\min} = 9$ ).

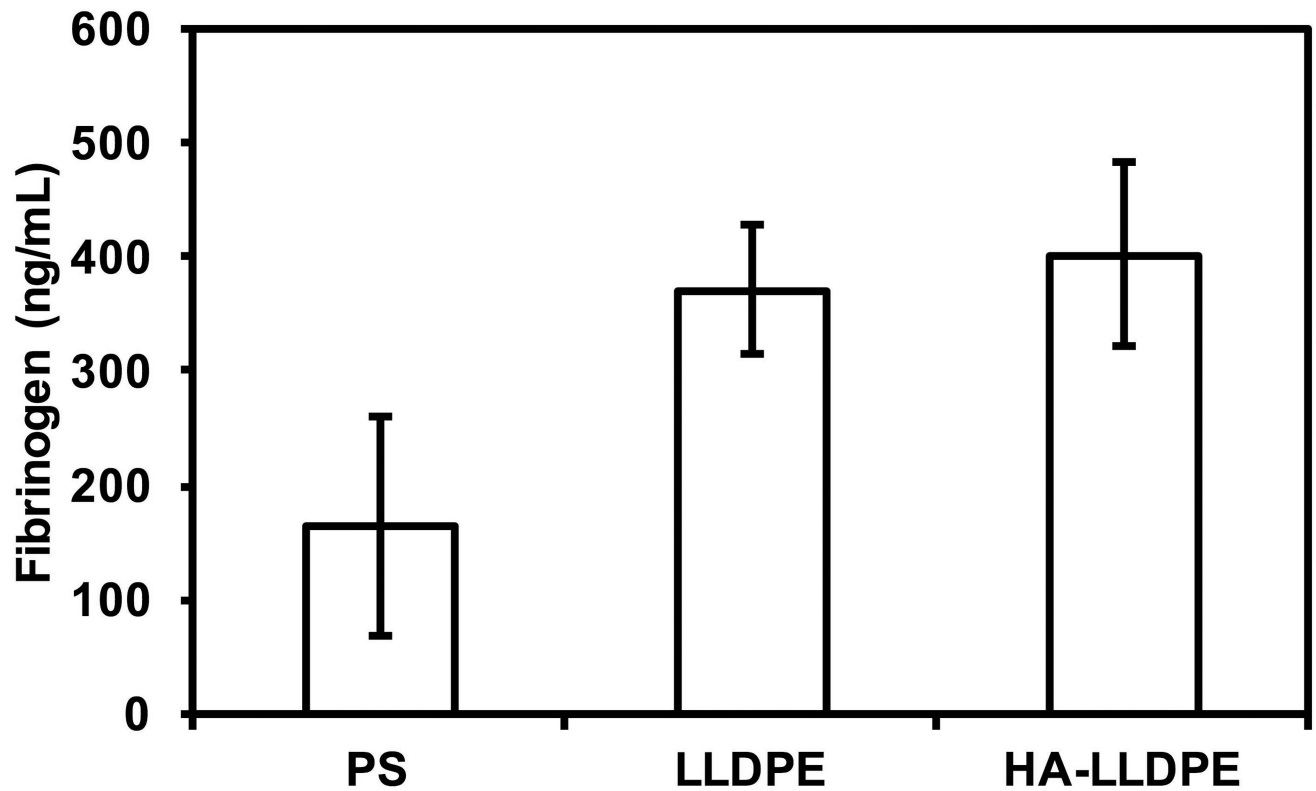


**Figure 5.**

Fibrinogen concentration measured in human plasma after 2 hrs of surface incubation in whole blood plasma. The results indicate a significantly higher concentration of fibrinogen bound to PS as indicated by less remaining fibrinogen in the plasma ( $p < 0.05$ ). No significant differences were seen in the binding of fibrinogen to LLDPE and HA-LLDPE surfaces, although overall trends pointed to less fibrinogen binding to HA-LLDPE surfaces. Experiments were replicated three times with three different cell populations on at least five different samples ( $n_{\min} = 15$ ).

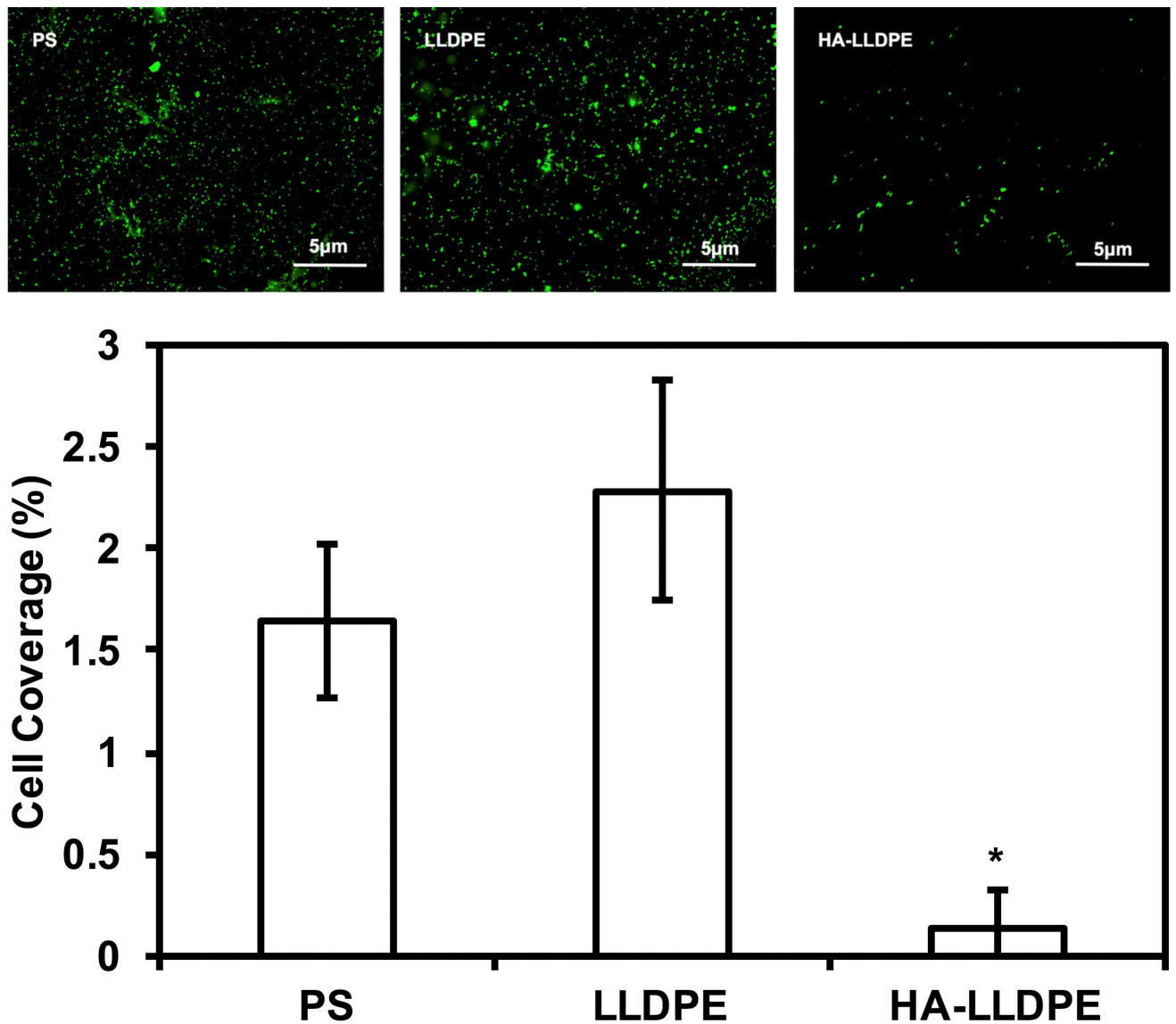
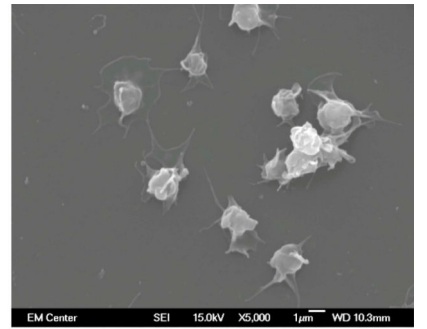
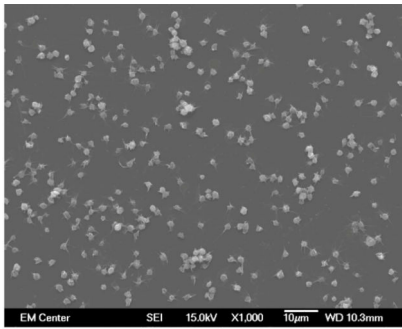
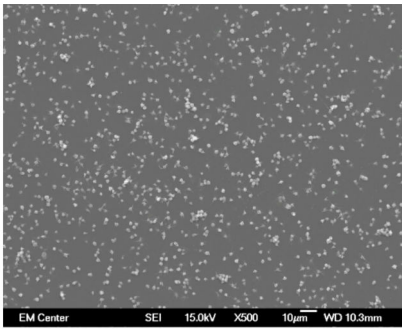


**Figure 6.**

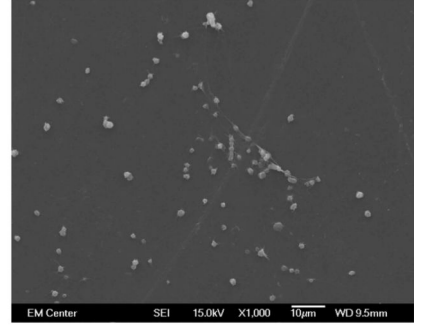
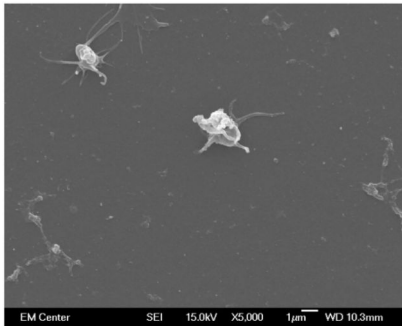
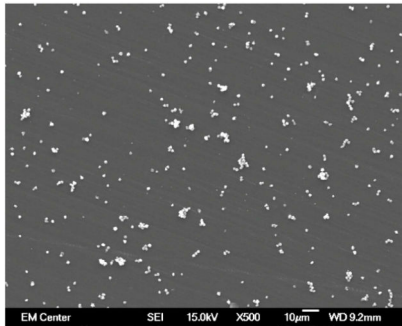
(a) Representative fluorescence microscopy images of adhered platelets and leukocytes stained with Calcein-AM on PS, LLDPE, and HA-LLDPE surfaces.

(b) Percent coverage analysis of adhered platelets and leukocytes after staining with Calcein-AM on PS, LLDPE, and HA-LLDPE surfaces. Percent coverage of platelets were determined by the evaluation of 15 representative images taken per group over 3 studies (n = 45) using ImageJ. Each image covered an area of 25 μm<sup>2</sup>. Results indicated significantly less cellular adhesion on HA-LLDPE as compared to other surfaces (p < 0.05).

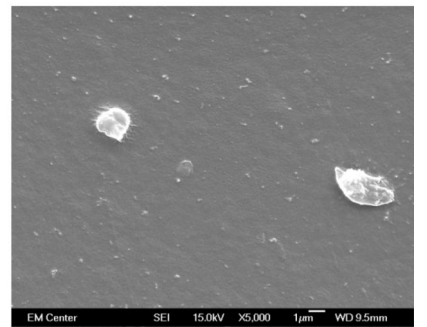
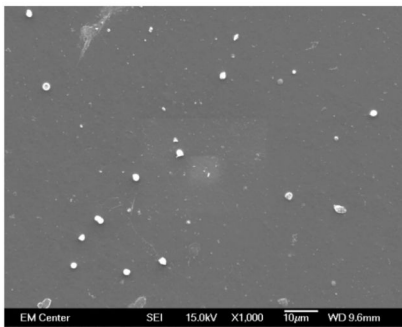
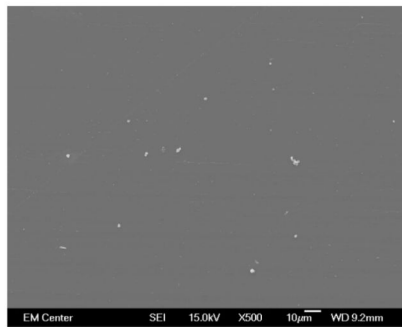
**PS**



**LLDPE**



**HA-LLDPE**





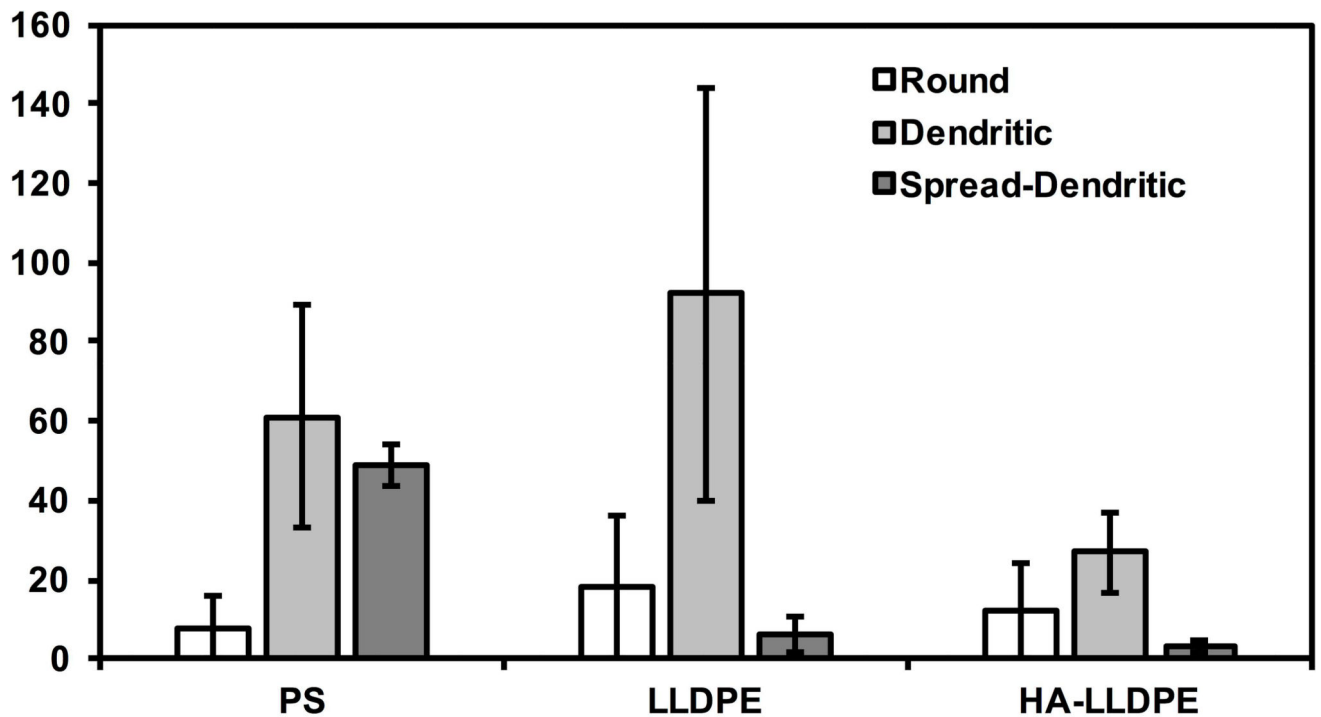


**Figure 7.**

(a) Representative SEM images of adhered platelets and leukocytes on PS, LLDPE, and HA-LLDPE surfaces. Results indicate HA-LLPE surfaces promoted no activation of platelets as noted by the rounded morphology. By comparison PS and LLDPE both resulted in fully activated platelets as expressed by the spread-dendritic morphology of platelets on these surfaces.

(b) Platelet count on different surfaces. Qualitative SEM analysis was performed using the methods described elsewhere on 15 representative images per group taken over 3 studies at 1000C (n = 45). Each image covered an area of 144  $\mu\text{m}^2$ . For HA-LLDPE, the number of un-activated platelets was significantly lower than dendritic and dendritic-spread platelets (p 0.05).

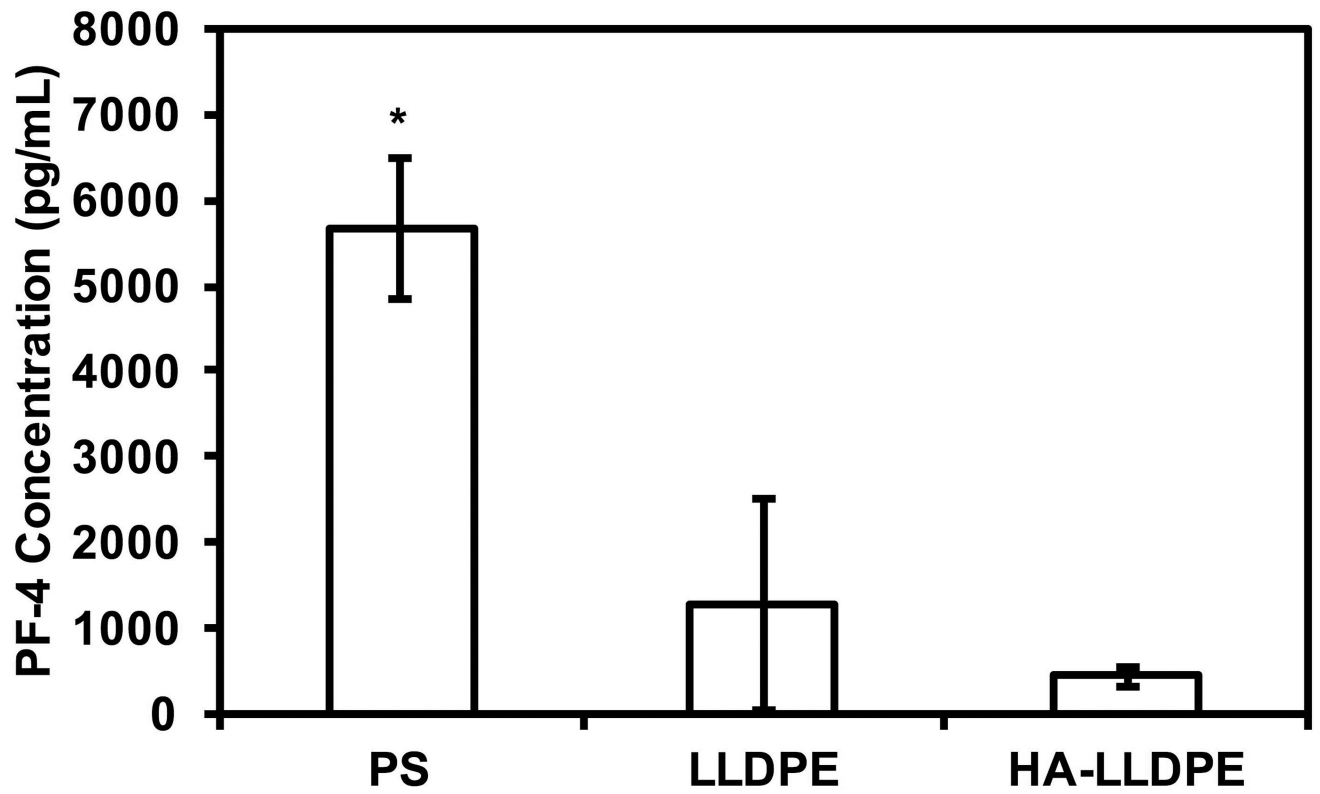


**Figure 8.**

PF-4 expression of degranulated platelets after 2 hrs of incubation in whole blood plasma. Results indicate a significant increase in PF-4 expression on PS surfaces compared to LLDPE and HA-LLDPE surfaces. Experiments were replicated with at least three different cell populations on at least three different samples ( $n_{\min} = 9$ ).

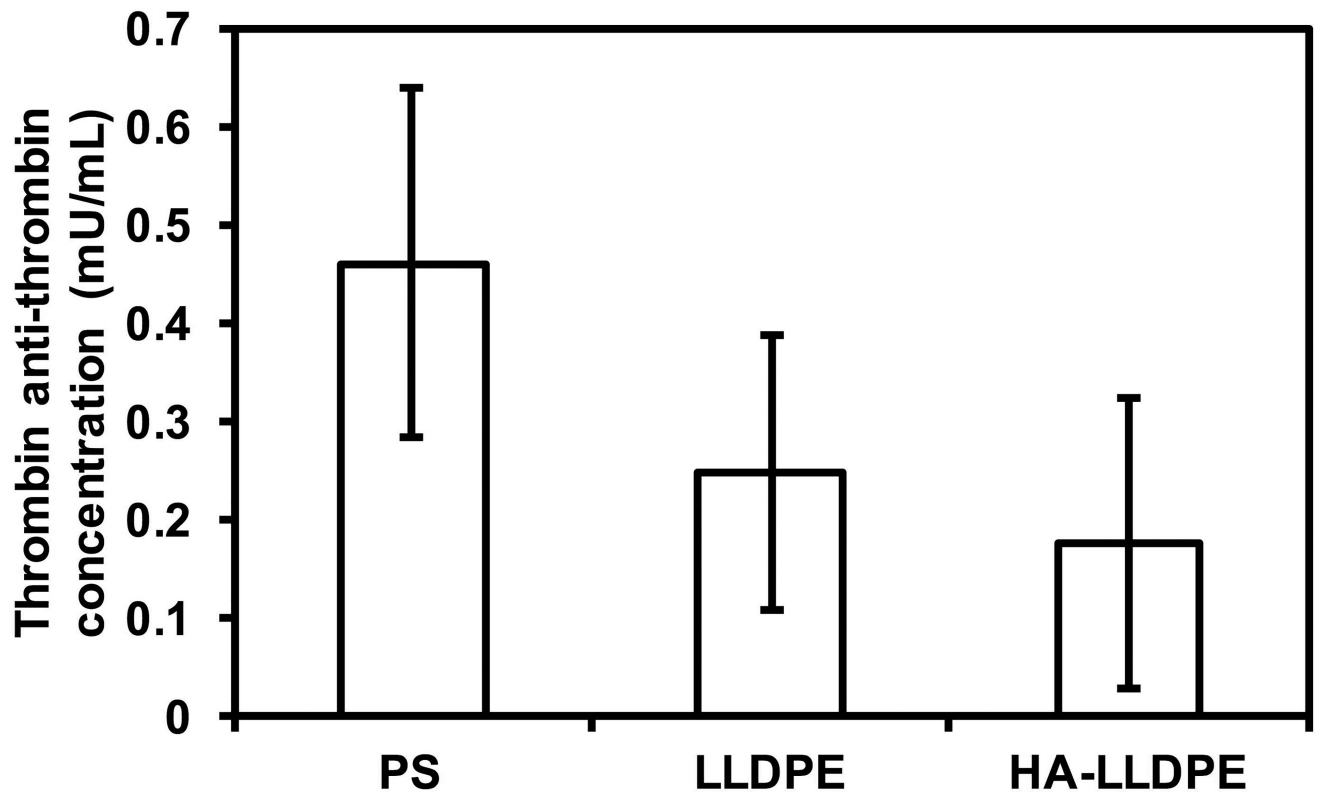


**Figure 9.**

TAT concentration determined after 2hrs of incubation of different surfaces in whole blood plasma. Results indicate no significant difference in TAT concentration on all the surfaces.